ISSN 2176-5480

22nd International Congress of Mechanical Engineering (COBEM 2013)
November 3-7, 2013, Ribeirão Preto, SP, Brazil

NUMERICAL STUDY OF THE SIMPLIFIED SET OF GLICKSMAN SCALING LAWS IN A CIRCULATING FLUIDIZED BED

Fabiano Anderson Pedroso
Flávia Zinani
Maria Luiza Sperb Indrusiak
Mechanical Engineering Graduate Program, Universidade do Vale do Rio dos Sinos, São Leopoldo, RS, Brazil.
fabianoanderson@unisinos.br, fzinani@unisinos.br, mlsperb@unisinos.br

Abstract. *The objective of this study is to verify the hydrodynamic similarity between two scales of a Circulating Fluidized Bed (CFB) reactor using computational fluid dynamics. Simplified set of Glicksman scaling parameters was used to build the model for a small scale reactor in an 1:4 scale. An Eulerian-Granular mathematical model was employed to describe the multiphase flows, using the computational dynamics code MFIX. For the real scale reactor, the model was validated using experimental results from the literature, and a mesh study was also performed. In order to validate hydrodynamic similarity between the two scales, vertical head loss profile, horizontal solids vertical velocity and solids density profiles were analyzed. Also, some perturbations in the particle size and superficial gas velocity were imposed in order to verify the stability of the scaled model. The numerical results showed that the scaled CFB presented a good hydrodynamic similarity with the real scale reactor. The perturbations imposed in particle size and gas superficial velocity implied in most cases in an increase of the mean relative error of hydrodynamic variables in relation to the CFB built with complete correspondence with the scaling laws.*

Keywords: *scaling laws, circulating fluidized bed, hydrodynamics, computational fluid dynamics.*

1. INTRODUCTION

Fluidized Bed Combustion (FBC) is a technology characterized by its ability to significantly reduce pollutant emissions compared to traditional methods of burning pulverized fuel. Currently, it can be considered a consolidated technological resource for generating energy by the combustion of coal, biomass and waste (Mukadi, *et al.,* 2000). In Brazil there is a potential for power generation in FB by the combustion of coal, given the large amount of available reserves, of which over 99% are concentrated in the states of Rio Grande do Sul and Santa Catarina (Agência Nacional de Energia Elétrica, 2008).

Fluidization is the process by which a liquid or gas flows through a particulate solid phase, keeping it under suspension, which caused the solid phase to have a fluid-like behavior (Kunii and Levenspiel, 1991). The interest in industrial applications of FBs is mainly due to the large contact between the solid and gaseous phases during fluidization.

Among applications involving FBs, there are the systems that use solids circulation in Circulating Fluidized Beds (CFB), due to the versatility of applications such as calcination, synthesis and decomposition of chemical compounds, coal combustion, gasification of biomass and coal, among others. These uses are favored by the benefits of technology-specific CFB as high reaction rate, ease of operational control and competitive construction cost.

Due to the need to develop a FB reactor on commercial scale operating with optimized parameters, it is necessary to build small-scale models that can predict the fluid dynamics of the reactor on a commercial scale (Yang, 1999). The techniques of scale are often complex and inaccurate, because they involve a mix of mathematical theories and historical considerations (Matsen, 1996). Historically, scaling laws were developed and systematically studied after the original work of Glicksman (1984), based on similarity methods, which allowed a more formal approach to the problem (Glicksman, *et al.*, 1994).

Together with the scaling laws, Computational Fluid Dynamics (CFD) applied to FBs can provide the necessary complementarity to assist in the demonstration of hydrodynamic similarity between scaled FBs (Knowlton *et al.*, 2005). In order to obtain a bi-univocal correspondence between numerical results of FBs scaled using the scaling laws of Glicksman, recently the numerical validation of scaling laws has been an important theme of research (Benyahia, *et al.,* 2005; Detamore, *et al.* 2001; Ommen, *et al.,* 2006; Sanderson, *et al.,* 2007).

The present study aimed to investigate the hydrodynamic similarity between the numerical results obtained from a numerical model implemented in the software MFIX for a CFB with dimensions of an actual prototype and a scaled CFB satisfying the simplified set of Glicksman scaling laws, using an Euler-Granular model to the gas-solid multiphase flow. The numerical results for the full-scale model were validated using experimental results of the Third Challenge NETL/PRSI (Challenge, 2010)

2. MATHEMATICAL MODELING

The equations described in this section are adapted from Syamlal, *et al.* (1993), the theory manual of the code MFIX, and "Summary of Equations MFIX 2012-1" by Benyahia, *et al.* (2012). For our modeling of multiphase flow an Euler-Granular approach was employed, which considers the solid and gaseous phases as interpenetrating continuous media, mapped with respect to a fixed reference point in space. The presence of each phase is described by the volume fraction occupied by the respective phase in each control volume. In this paper, only a gas phase and a solid phase are considered, for which the mass and momentum balances are applied separately.

2.1 Mass Balance Equations

Using an Eulerian modeling, the mass balance over a control volume is described by the continuity equation for each phase composing the system. Eq. (1) and Eq. (2) represent the mass balance for the gas and solid phases, respectively:

$$\frac{\partial}{\partial t}\left(\varepsilon_g\rho_g\right)+\nabla\left(\varepsilon_g\rho_g\boldsymbol{u}_g\right)=0 \tag{1}$$

$$\frac{\partial}{\partial t}\left(\varepsilon_s\rho_s\right)+\nabla\left(\varepsilon_s\rho_s\boldsymbol{u}_s\right)=0 \tag{2}$$

where t is the time, ε_g the gas volume fraction, ε_s the solid volume fraction, ρ_g the gas mass density, ρ_s the solid mass density, ∇ the nabla operator, $\boldsymbol{u}_g$ the gas velocity vector and $\boldsymbol{u}_s$ the solid velocity vector.

2.2 Momentum Balance Equations

The momentum balance for a control volume is obtained using Newton second law. For the gas phase, it is represented by Eq. (3) and for the solid phase by Eq. (4),

$$\frac{\partial}{\partial t}\left(\varepsilon_g\rho_g\boldsymbol{u}_g\right)+\nabla\left(\varepsilon_g\rho_g\boldsymbol{u}_g\boldsymbol{u}_g\right)=\nabla\boldsymbol{\tau}_g-\varepsilon_g\nabla P+\varepsilon_g\rho_g\boldsymbol{g}-\boldsymbol{I} \tag{3}$$

$$\frac{\partial}{\partial t}\left(\varepsilon_s\rho_s\boldsymbol{u}_s\right)+\nabla\left(\varepsilon_s\rho_p\boldsymbol{u}_s\right)=\nabla\boldsymbol{\tau}_s-\varepsilon_s\nabla P+\varepsilon_s\rho_s\boldsymbol{g}-\boldsymbol{I} \tag{4}$$

where $\boldsymbol{\tau}$ is the extra stress tensor for each phase, P the gas pressure and $\boldsymbol{I}$ the vector of interaction forces which result from momentum transfer among phases. It is given by Eq. (5),

$$\boldsymbol{I}=\beta\left(\boldsymbol{u}_g-\boldsymbol{u}_s\right) \tag{5}$$

where the drag coefficiet β is obtained from a correlation, as the one of Gidaspow.

In Gidaspow drag model, the dense phase, when $\varepsilon_s > 0.2$, is modeled using Ergun equation (Ergun, 1952) and the disperse phase, when $\varepsilon_s \leq 0.2$, using the Wen and Yu (1966) model, as follows in Eq. (6):

$$\beta=\begin{cases}150\dfrac{\varepsilon_s^2\mu}{\varepsilon_g d_p^2}+1.75\dfrac{\varepsilon_s\rho_g\left|\boldsymbol{u}_s-\boldsymbol{u}_g\right|}{d_p} & \text{if} \quad \varepsilon_s>0,2\\[2ex] \dfrac{3}{4}C_d\varepsilon_g^{2.65}\dfrac{\varepsilon_s\varepsilon_g\rho_g\left|\boldsymbol{u}_s-\boldsymbol{u}_g\right|}{d_p} & \text{if} \quad \varepsilon_s\leq 0.2\end{cases} \tag{6}$$

where μ is the gas dynamic viscosity and d_p the particle diameter,

$$C_d=\begin{cases}\dfrac{24}{Re}\left(1+0.15Re^{0.687}\right) & \text{if} \quad Re<1000\\ 0.44 & \text{if} \quad Re\geq 1000\end{cases} \tag{7}$$

and

ISSN 2176-5480

$$Re=\frac{\rho_g|\boldsymbol{u}_s-\boldsymbol{u}_g|d_p}{\mu} \tag{8}$$

is the Reynolds number based on the particle diameter.

The gas phase extra stress tensor is that of a Newtonian fluid, Eq. (9):

$$\boldsymbol{\tau}_g=2\mu\boldsymbol{D}_g \tag{9}$$

where

$$\boldsymbol{D}_g=\frac{1}{2}\left[\nabla\boldsymbol{u}_g+\left(\nabla\boldsymbol{u}_g\right)^T\right]-\frac{1}{3}\nabla\boldsymbol{u}_g\boldsymbol{\delta} \tag{10}$$

is the strain rate tensor and $\boldsymbol{\delta}$ the unitary tensor.

The gas is considered as a perfect gas, while the solid phase is modeled after the Kinetic Theory of Granular Flows (KTGF)

2.3 Kinetic Theory of Granular Flow

The KTGF is an analogy between the granular flows and the kinetic theory of gases, and provides the basis for describing the stress tensor of the solid phase in the Euler-Granular model. The granular temperature, Θ, given by

$$\frac{3}{2}\Theta_s=\frac{1}{2}\boldsymbol{C}^2 \tag{11}$$

is the specific kinetic energy of the random fluctuating component of the particle velocity, where $\boldsymbol{C}$ is the fluctuating component of the instantaneous velocity, $\boldsymbol{c}$, defined by Eq. (12):

$$\boldsymbol{c}=\boldsymbol{u}_s+\boldsymbol{C} \tag{12}$$

The granular energy transport is given by Eq. (13):

$$\frac{3}{2}\varepsilon_s\rho_s\left(\frac{\partial\Theta_s}{\partial t}+\boldsymbol{u}_s\cdot\nabla\Theta_s\right)=\left(\boldsymbol{D}_s:\nabla\boldsymbol{u}_s-\nabla\cdot\boldsymbol{q}_\Theta-\gamma_\Theta+\phi_{gs}\right) \tag{13}$$

where the rate of dissipation of granular energy due to inelastic, γ_Θ, is given by Eq. (14) and the diffusive flux of granular energy, $\boldsymbol{q}_\Theta$, is defined by Eq. (15).

$$\gamma_\Theta=k_4\varepsilon_s^2\Theta^{\frac{3}{2}} \tag{14}$$

$$\boldsymbol{q}_\Theta=-k_\Theta\nabla\Theta \tag{15}$$

The kinetic and collisional terms are neglected, and the coefficient of granular energy diffusion, k_Θ, is defined by Eq. (16):

$$k_\Theta=\frac{15d_p\rho_s\varepsilon_s\sqrt{\pi\Theta}}{4(41-33\eta)}\left[1+\frac{12}{5}\eta^2(4\eta-3)\varepsilon_s g_0+\frac{16}{15\pi}(41-33\eta)\eta\varepsilon_s g_0\right] \tag{16}$$

where

$$\eta=\frac{1-e}{2} \tag{17}$$

and g_0 is the radial distribution function, given by Eq. (18):

$$g_0=\frac{1-0.5\varepsilon_s}{(1-\varepsilon_s)^3} \tag{18}$$

and

ISSN 2176-5480

$$k_4=\frac{12(1-e^2)\rho_s g_0}{d_p\sqrt{\pi}} \tag{19}$$

The term ϕ_{gs} represents the transfer of granular energy from the gas phase to the solid phase, it is defined by Eq. (20):

$$\phi_{gs}=-3F_{gs}\Theta \tag{20}$$

where F_{gs} is the coefficient of the interaction force between the gas and solid phases.

The solid stress tensor, $\boldsymbol{\tau}_s$, is given by Eq. (21):

$$\boldsymbol{\tau}_s=\left(-P_s+\eta\mu_b\nabla\boldsymbol{u}_s\right)\boldsymbol{I}+2\mu_s\boldsymbol{D}_s \tag{21}$$

where

$$\boldsymbol{D}_s=\frac{1}{2}[\nabla\boldsymbol{u}_s+(\nabla\boldsymbol{u}_s)^T]-\frac{1}{3}\nabla\boldsymbol{u}_s\boldsymbol{I} \tag{22}$$

and for the solid pressure, P_s,

$$P_s=\varepsilon_s\rho_s\Theta_s\left(1+4g_0\varepsilon_s\eta\right) \tag{23}$$

with μ_s the solid viscosity defined by Eq. (24):

$$\mu_s=\left(\frac{2+\alpha}{3}\right)\left\{\frac{\mu_s^*}{g_0\eta(2-\eta)}\left(1+\frac{8}{5}\eta g_0\varepsilon_s\right)\left[1+\frac{8}{5}\eta(3\eta-2)g_0\varepsilon_s\right]+\frac{3}{5}\eta\mu_b\right\} \tag{24}$$

where

$$\mu_s^*=\frac{\varepsilon_s\rho_s\Theta_s g_0\mu}{\varepsilon_s\rho_s\Theta_s g_0+\frac{2\beta\mu}{\varepsilon_s\rho_s}} \tag{25}$$

$$\mu=\frac{5}{96}\rho_s d_p\sqrt{\pi\Theta_s} \tag{26}$$

$$\mu_b=\frac{256}{5\pi}\mu\varepsilon_s^2 g_0 \tag{27}$$

This model is used in the viscous regime. In the plastic regime, the Schaeffer model is applied. In this case the viscosity of the solids in the plastic regime is determined by Eq. (28) and the pressure of the solids in the plastic regime by Eq. (29),

$$\mu_{sp}=\frac{P_{sf}\sin\phi_\alpha}{2\sqrt{I_{2D}}} \tag{28}$$

$$P_{sp}=\begin{cases}10^{24}\left(\varepsilon_s-\varepsilon_s^*\right)^2 & \text{if } \varepsilon_s>\varepsilon_s^* \\ 0 & \text{if } \varepsilon_s\leq\varepsilon_s^*\end{cases} \tag{29}$$

3. GLICKSMAN SCALING LAWS

The development of a new commercial unit of a FB requires the construction of a small scale reactor before the building the commercial scale plant. If hydrodynamic similarity among the scales is guaranteed, the scaled bed can be used to improve performance and accurately predict the operating conditions of the full scale prototype (Glicksman, 1999). Fluidized beds are considered to be hydrodynamically similar if they have a good correspondence (qualitatively and quantitatively) among the main fluid dynamic variables, such as gas pressure, gas and solids velocity and volume fraction fields across the reactors.

ISSN 2176-5480

3.1 Full Set of Glicksman Scaling Laws

Departing from the equations of motion and continuity for solid and gaseous phases and making use of dimensional analysis, Glicksman (1984) proposed his first set of dimensionless independent parameters to be used to build equivalent FB, hydrodynamically similar. As a prerequisite, it requires geometric similarity between scales, so that all spatial dimensions are correlated by the same scale factor and the angles are preserved. Fluidized beds are to present hidrodynamic similar behavior when geometric similarity is presented and all relevant independent dimensionless parameters are identical between scaled beds.

The full set of Glicksman parameters, ψ, is given by Eq. (30), where D is the diameter of the bed, L the bed height, u_0 the gas superficial velocity, G_s the solids mass flux, φ the sphericity of the particles and BD the bed dimensions.

$$\psi=\psi\left[\frac{u_0^2}{gD}, \frac{\rho_g}{\rho_s}, \frac{\rho_s u_0 d_p}{\mu}, \frac{\rho_g u_0 L}{\mu}, \frac{G_s}{\rho_s u_0}, \varphi, BD\right] \tag{30}$$

3.2 Simplified Set of Glicksman Scaling Laws

Because there are five hydrodynamic parameters (besides geometrical parameters ϕ and BD) in the full set of Glicksman scaling laws, there are considerable limitations on the flexibility of sizing FBs, since the similarity requires that all parameters are met. Thus, modeling a scaled FB according to the complete set requires a unique combination of solids mass density, particle diameter and bed dimensions.

As an example of the difficulty to model a scaled FB using the full set of dimensionless parameters (Rüdsüli, 2012), consider a FB of 1.6 m in diameter operating at 320 °C and 250 kPa. To be modeled on a laboratory scale of 0.2 m the particle density should be of 23,000 kg/m³ and the pressure equal to 2,000 kPa. Such conditions are impractical.

Glicksman, *et al.* (1993) proposed a simplification of scaling laws in a set composed of only four dimensionless hydrodynamic parameters, allowing greater freedom in defining operational parameters. That is obtained by simplifying the Ergun equation for conditions where the drag is either dominated by viscous or inertial forces. The simplified set of Glicksman is shown in Eq. (31).

$$\psi=\psi\left[\frac{u_0^2}{gD}, \frac{\rho_s}{\rho_g}, \frac{u_0}{u_{mf}}, \frac{G_s}{\rho_s u_0}, \varphi, BD\right] \tag{31}$$

4. NUMERICAL MODELING AND SIMULATIONS

To represent the geometry of the CFB in question, a two-dimensional adaptation of the real model was designed. Figure 1 displays the geometries constructed for the numerical modeling, which was limited to model only the part of the ascending column corresponding to the region between the distributor and the top of the reactor. Only one significant geometric adaptation was applied to the inlet and outlet of the solid bed. In the experimental model the entrance and exit of the solid occurred in only one point on respectively bottom and top region of the riser. The use of a two-dimensional model that faithfully represents this type of geometry, tend to present asymmetric horizontal profiles (Chalermsinsuwan, *et al.,* 2009). Thus, the input and output of the solid bed were doubled in opposite and symmetrical side points and the total crossing area has been preserved, having been used at one half the original area for each input and output side of the model.

ISSN 2176-5480

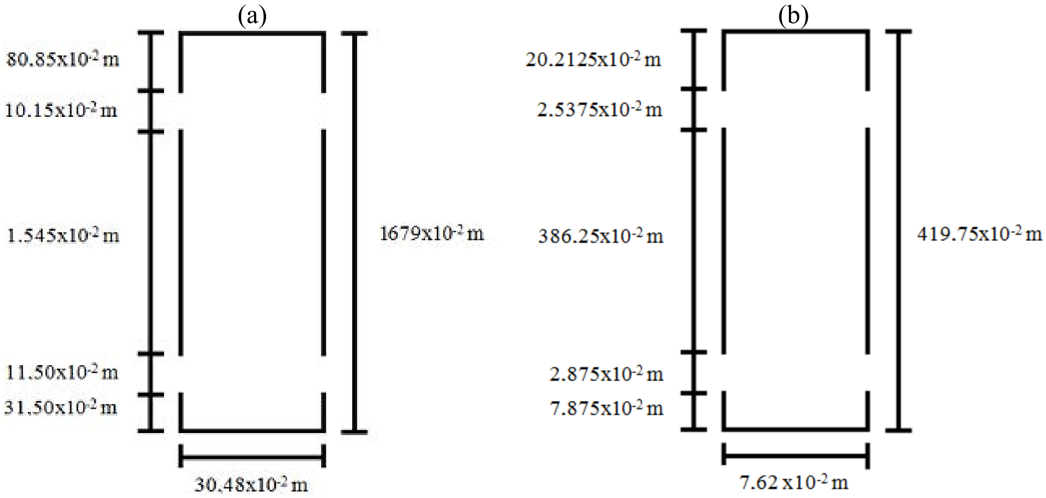

Figure 1. Geometric model used in the simulations for the full-scale bed (a) and scaled bed (b).

A summary of the main parameters of the numerical model implemented for the full-scale beds (Bed 1) and scaled bed according to simplified set of Glicksman scaling laws (Bed 2), is shown in Tabs. 1 and 2, where e_w is the wall coefficient of restitution and e the interparticle coefficient of restitution, NCV is the number of control volumes and t_{max} the total time of simulation. All profiles analyzed were obtained from time averaged results taken over the last 70 s for the Bed 1 and 35 s for the Beds 2-6.

Table 1. Variables and parameters used in numerical simulations of beds in full-scale and scaled according to simplified set of Glicksman scaling laws

Variable / Parameter	Real Bed - Bed 1	Scaled Bed - Bed 2
d_p	802×10^{-6} m	545.7×10^{-6} m
u_0	7.58 m/s	3.79 m/s
e_w	0.7	0.7
e	0.8	0.8
NCV	22539	22539
t_{max}	110 s	55 s

Table 2. Breakdown of operating parameters changed in beds built in mismatch with the simplified set of Glicksman scaling laws.

Bed	d_p	u_0
Bed 3	673.85×10^{-6} m	3.79 m/s
Bed 4	417.55×10^{-6} m	3.79 m/s
Bed 5	545.7×10^{-6} m	5.685 m/s
Bed 6	545.7×10^{-6} m	1.895 m/s

4.1 Experimental Validation

The experimental validation of the numerical model was made based on the experimental data of Case 4 of the Third Challenge NETL/PRSI (Challenge, 2010). This experiment relates to a CFB system operating in core-annular regime and particles belonging to Geldart Group B (Geldart, 1973). The profiles selected for validation were based on experimental data available. They were the horizontal profiles of solids vertical velocity and solids mass flux in a distance of 8.88 m from the bottom of the reactor.

It can be observed in Figure 2 a good match for the qualitative results of both profiles analyzed. Quantitatively, in the horizontal profile of solids vertical velocity, the mean relative error exceeding the range of 95% of the experimental results was 4%, while for the solids mass flux profile an error of 10% was obtained. Such range of values is acceptable in the numerical simulation of these types of systems (Li, *et al.* 2012).

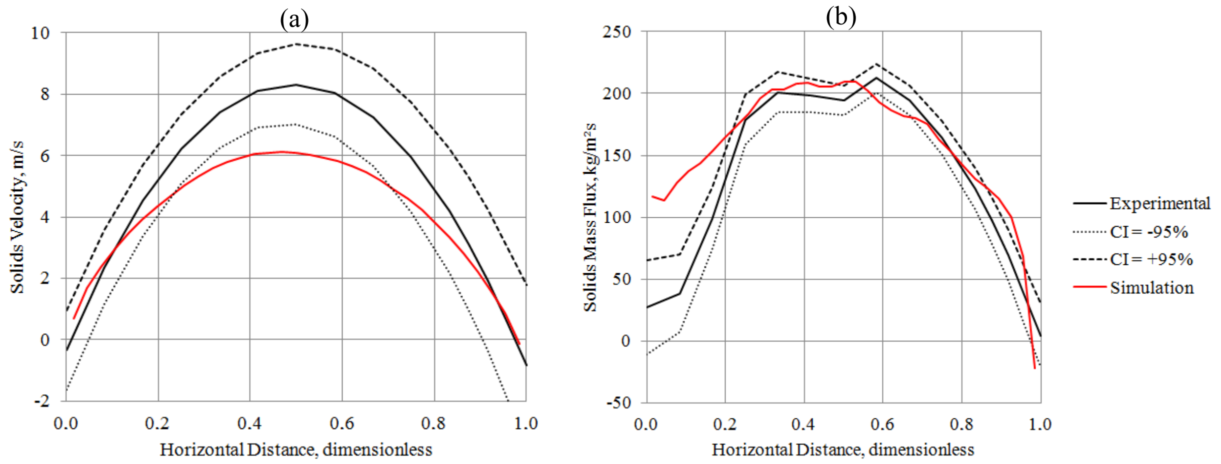

Figure 2. Experimental validation of the numerical model for the full-scale reactor. Horizontal profile of the vertical solids velocity (a) and solids mass flux (b). CI is the confidence interval of 95% for the experimental data. Elevation of 8.88 m in bed.

5. RESULTS AND DISCUSSION

In order to verify the hydrodynamic similarity between data of the full-scale bed (Bed 1) and scaled bed constructed in accordance with the simplified set of Glicksman scaling laws (Bed 2), data for the horizontal dimensionless profiles d of solids density and solids vertical velocity at an elevation of 8.4 m were compared. These data were also compared to those obtained for beds scaled with changed operating parameters (Table 2).

Figure 3 shows the results for the horizontal profiles of dimensionless solids density. It is possible to observe that, qualitatively, Bed 2 showed a good similarity to Bed 1. For the data obtained with Beds 3-6, scaled with changes from the simplified set, one can observe a considerable deviation from the behavior of Bed 1.

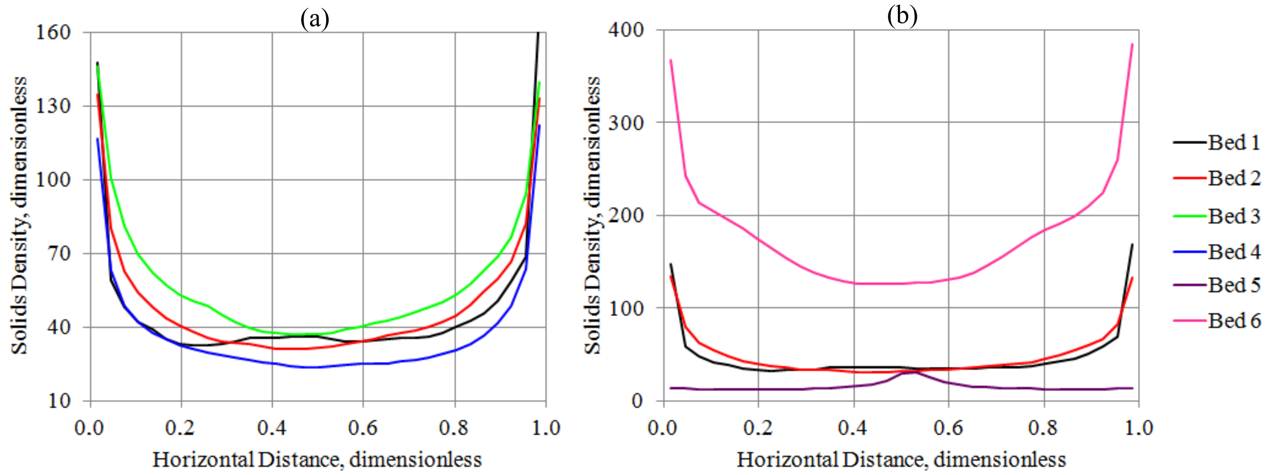

Figure 3. Comparison between the horizontal profiles of solids mass density. Real, scaled and change in particle diameter (a). Real, scaled and change in superficial gas velocity (b). Elevation of 8.4 m.

Figure 4 shows the results for the comparison of the horizontal profiles of the dimensionless vertical solids velocity. It is possible to observe that, qualitatively, Bed 2 showed a good similarity to Bed 1. For data obtained by beds with mismatched parameters for the particle diameter and superficial gas velocity, one can observe a significant deviation from the behavior of Bed 1, except for Bed 4 (particle diameter reduced), which exhibited a better qualitative match than Bed 2.

ISSN 2176-5480

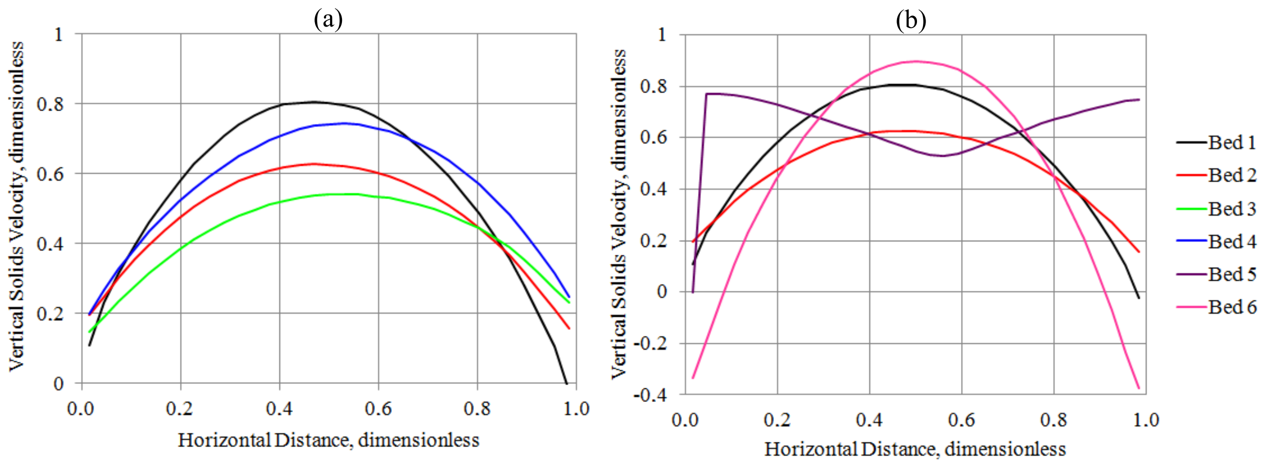

Figure 4. Comparison between the horizontal profiles of vertical velocity. Real, scaled and change in particle diameter (a). Real, scaled and change in superficial gas velocity (b). Elevation of 8.4 m.

Figure 5 shows the results of the comparison of vertical profiles of pressure loss. It is possible to observe that, qualitatively, Bed 2 showed a good similarity to Bed 1. For the data obtained with the non-corresponding parameters beds (considering particle diameter and superficial gas velocity), one can observe a larger deviation from the behavior of Bed 1, especially by Bed 6, except for Bed 4 (particle diameter reduced), which exhibited a better qualitative match than Bed 2.

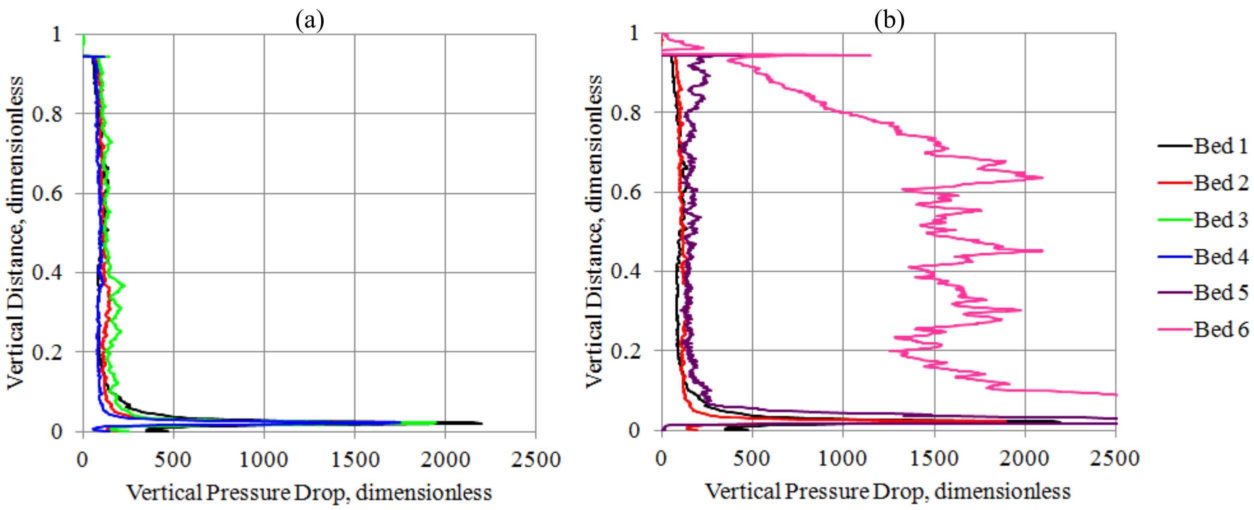

Figure 5. Comparison between vertical profiles of pressure drop between the beds. Real, scaled and change in particle diameter (a). Real, scaled and change superficial gas velocity (b).

Table 3 summarizes the average relative errors obtained for each profile of each simulation performed. It is possible to check that the bed scaled by the simplified set presented a reasonable quantitative similarity in relation to the full-scale bed, keeping the error below 22% for all profiles analyzed. It can also be seen that the beds built with changes in parameters, in general, presented a higher error, except for the Bed 4, which presented a smaller error in two of the three parameters analyzed.

Table 3. Average relative error for the analyzed profiles of beds scaled according to the simplified set of Glicksman and beds scaled with changed parameters. Errors relative to the numerical results for the full-scale unit.

Variables, dimensionless	Bed 2	Bed 3	Bed 4	Bed 5	Bed 6
Solids Density	0.87%	1.66%	1.16%	4.02%	16.34%
Vertical Solids Velocity	20.11%	31.23%	13.74%	47.64%	25.86%
Vertical Pressure Drop	21.78%	39.41%	16.55%	51.26%	1,236.97%

6. CONCLUSIONS

From the qualitative and quantitative analysis of some hydrodynamic profiles, it was observed that for the case under consideration, the CFB operating under core annulus regime scaled according to the simplified set of Glicksman scaling laws can reproduce with reasonable accuracy the results of a full-scale unit. Additionally it was found that a reduction in the diameter of the particle in the scaled bed produced more satisfactory results for some of the profiles analyzed. It is suggested that this result is due to a greater correspondence among parameter d_p/D, implicitly contained in the full set of Glicksman scaling laws.

7. ACKNOWLEDGEMENTS

We acknowledge the agency CAPES - Brazil for financial support through the concession of a scholarship to F. Pedroso and for project PNPD 2010. The author F. Zinani is a grant holder of CNPq - Brazil.

8. REFERENCES

Agência Nacional De Energia Elétrica, 2008. “Atlas de Energia Elétrica do Brasil”. 16 jan. 2013. <http://www.aneel.gov.br/arquivos/PDF/atlas3ed.pdf>.

Benyahia, S.; Pannala, S.; Finney, C.E.A.; Syamlal, M., Dow, S.C.; O’Brien, T., 2005. “Computational Validation of the Glicksman Scaling Laws Using Gas/Solids Fluidized Bed Simulations”. In: *AIChE Annual Meeting*, USA.

Benyahia, S.; Syamlal, M.; O’Brien, T.J., 2012. “Summary of MFIX Equations 2012-1”. 20 mar. <https://mfix.netl.doe.gov/documentation/MFIXEquations2012-1.pdf>.

Challenge, 2010. “Third Challenge PSRI/NETL”. 2 jan. 2013. <https://mfix.netl.doe.gov/challenge/index_2010.php>.

Chalermsinsuwan, B.; Chanchuey, T.; Buakhao, W.; Gidaspow, D.; Piumsomboon, P., 2012. “Computational fluid dynamics of circulating fluidized bed downer: Study of modeling parameters and system hydrodynamic characteristics”. *Chemical Engineering Journal*, V. 189-190, p. 314-335.

Detamore, M.S.; Swanson, M.A.; Frender, K.R.; Hrenya, C.M., 2001. “A kinetic-theory analysis of the scale-up of circulating fluidized beds”. *Powder Technology*, V. 116, p. 190-203.

Ergun, S., 1952. “Fluid Flow Through Packed Columns”. *Chemical Engineering Progress*, V. 48, p. 89-94.

Glicksman, L.R., 1984. “Scaling Relationship for Fluidized Beds”. *Chemical Engineering Science*, V. 39, p. 1373-1379.

Jackson, R., 1971. Fluid Mechanical Theory. In: DAVIDSON, J.F.; HARRISON, D., Fluidization. Academic Press, London.

Glicksman, L.R., 1999. “Fluidized Bed Scale-up”. In: YANG, Wen-Ching. *Fluidization, Solid Handling and Process*. Noyes Publications, Westwood.

Glicksman, L.R.; Hyre, M.R.; Farrel, P.A., 1994. “Dynamic Similarity in Fluidization”. *International Journal of Multiphase Flow*, V. 20, p. 331-386.

Knowlton, T.M.; Karri, S.B.R.; Issangya, A., 2005. “Scale-up of Fluidized-Bed Hydrodynamics”. *Powder Technology*, v. 150, p. 72-77.

Kunii, D.; Levenspiel, O., 1999. *Fluidization Engineering*. Butterworth-Heinemann, Newton.

Li, T.; Dietiker, J.F.; Shahnam, M., 2012. “MFIX Simulation of NETL/PSRI challenge problem of circulating fluidized bed”. *Chemical Engineering Science*, V. 84, p. 746-760.

Matsen, J.M., 1996. “Scale-up of fluidized bed processes: principle and practice”. *Powder Technology*, V. 88, p. 237-244.

Mukadi, L.; Guy, C.; Legros, R., 2000. “Prediction of Gas Emissions in an Internally Circulating Fluidized Bed Combustor for Treatment of Industrial Solid Wastes”. *Fuel*, V. 79, p. 1125-1136.

Ommen, J. R.; Teuling, M.; Nijenhuis, J.; Wachem, B. G. M., 2006. “Computational validation of the scaling rules for fluidized bed”. *Powder Technology*, v. 163, p. 32-40.

Rüdisüli, M.; Schildhauer, T.J.; Biollaz, S.M.A.; Ommen, J. R., 2012. “Scale-up of bubbling fluidized bed reactor - A review”. *Powder Technology*, V. 217, p. 21-38.

Sanderson, J.; Wang, X.S.; Rhodes, M.J.; Lim, K. S., 2007. “An investigation of fluidized bed scaling laws by DEM simulation”. In: *The 12th International Conference on Fluidization - New Horizons in Fluidization Engineering*, Vancouver, Canada.

Syamlal, M., Rogers, W., O’Brien, T., 1993. “MFIX documentation: theory guide. Technical Note, DOE/METC-94/1004”, U.S. Department of Energy, USA.

Wen, Y.C., Yu, Y.H., 1966. “Mechanics of fluidization”. *Chemical Engineering Progress Symposium Series*. V. 62, p. 100-111.

Yang, W.C., 1999. *Fluidization, Solid Handling and Process*. Noyes Publications, Westwood.

9. RESPONSIBILITY NOTICE

The authors are the only responsible for the printed material included in this paper.